Constraints on the G1/S transition pathway may favor selection of multicellularity as a passenger phenotype

Selection of multicellularity as a passenger phenotype

Tom Louis Ducrocq, Damien Laporte and Bertrand Daignan-Fornier*

Univ. Bordeaux, CNRS, IBGC, UMR 5095, F-33000 Bordeaux, France

ORCID : TLD (0009-0009-6148-4057); DL (0000-0002-1556-5253); BDF (0000-0003-2352-9700)

*Corresponding author

bertrand.daignan-fornier@u-bordeaux.fr

Abstract

Multicellularity has emerged in the three branches of the tree of life. The formation of simple multicellular entities can either result from cells aggregating or staying together after mitosis. However, it is not yet fully understood how, once formed, these simple multicellular entities could be maintained or even selected for. Here, using the *ace2* yeast snowflake model of simple multicellularity, we aimed at identifying genetic conditions favoring its maintenance. Growth-competition experiments revealed that, while the *ace2* mutation by itself does not provide any fitness advantage or disadvantage, the *ace2* snowflakes were strongly selected when combined to conditions affecting regulators of the G1/S transition of the cell cycle, such as Cln3 or Whi5. We show that this selection results from a faster exit from quiescence of the *ace2* snowflake cells. Importantly, this advantage is not dependent on the multicellular phenotype, but rather on the *ace2* genotype itself. We found that the *ace2* selective advantage in the *cln3* background fully depends on the *KSS1* gene, a target of the Ace2 transcription factor. Finally, we show that phenotypes observed for *ace2* mutants are phenocopied by the $AMN1^{368D}$ allelic form found in "non-laboratory" yeast strains, hence adding physiological relevance to these observations. Altogether, our results support the hypothesis that simple multicellularity could, in some cases, persist, not because it provides a direct selective advantage due to multicellularity itself, but rather as a "passenger" phenotype that is maintained alongside other selected traits.

Introduction

Multicellularity has evolved repeatedly and independently in distinct lineages within bacteria, archaea and eukaryotes (1). This evolutionary process firstly involves the selection of simple forms of multicellularity such as clusters of cells. Several selective drivers of simple multicellularity have been proposed (2) that are generally associated to changes in geometry allowing access to new resources (faster sedimentation, increased mobility, foraging, dispersal), as well as other advantages associated with size increase (predation avoidance, stress resistance, improved extracellular metabolism) and finally, chimerism: the capacity to combine different cellular phenotypes in a single entity, allowing the establishment of intra-organism division of labor.

Many forms of multicellularity are facultative and their formation is triggered by external signals. One of the best studied case is that of the slime mold *Dictyostelium discoideum*, which cells, in response to resource limitation, aggregate to form a fruiting body that favors dispersal of spores (3,4). Another example comes from *Saccharomyces cerevisiae* cells that, under poor nitrogen conditions, can become highly polarized and stay attached, thereby favoring foraging, a phenomenon known as pseudohyphal growth (5,6). In such cases, multicellularity provides alternative options to the non-proliferation observed in unicellular organisms in response to local nutritional starvation (7). These multicellularity-specific responses are triggered by nutritional cues and, some of them may have evolved by functional recruitment of unicellular pre-existing sensors and pathways. It is hence likely that some actors of nutritional control of cell cycle progression should modulate facultative multicellularity. Indeed, there are several experimental evidences connecting the regulators of G1/S transition in the cell cycle to multicellularity. As described below for several species, this mostly concerns two major regulators, retinoblastoma (RB) and Cyclin D. RB is a negative regulator of E2F, a transcription factor critical for G1/S progression, while cyclin D is a negative regulator of RB (8).

Several experimental evidences connect regulators of G1/S transition, and notably RB, to multicellularity. First, when RB from the simple multicellular volvocine *Gonium pectorale* was

53 expressed in its close unicellular relative *Chlamydomonas*, the C*hlamydomonas* cells behaved as a
54 simple multicellular colonial entity (9). This points to an important role for RB in triggering uni- to
55 multicellular transition. Second, in the aggregative multicellular slime mold, *Dictyostelium discoideum*,
56 the RB orthologue, RblA, was found to be involved in the stalk *vs* spore cell-fate preference (10). Finally,
57 another key regulator of G1/S transition, namely Cyclin D, has also been associated to uni- to
58 multicellular transition in two different yeast species, *Candida albicans* and *Saccharomyces cerevisiae*
59 (11,12). Depending on environmental conditions, *Candida albicans* can grow either as a yeast
60 unicellular planktonic form, or as a multicellular hyphal form (13). The transition from one form to the
61 other is associated with invasion and virulence. Strikingly, the knock-down of the *C. albicans* cyclin D
62 orthologue Cln3 resulted in hyphal growth suggesting that the G1 phase of the cell cycle is important
63 in the transition from uni- to multicellular development in *C. albicans* (11). Similarly, in *S. cerevisiae*
64 deletion of *CLN3*, the budding yeast cyclin D homolog, enhanced pseudohyphal growth (12).
65 Interestingly, *CLN3* encodes an inhibitor of Whi5 which is the yeast functional equivalent of RB (13). It
66 hence seems that, during evolution, uni- to multicellularity transitions have repeatedly used pre-
67 existing regulators of the G1/S transition, such as RB and cyclin D. These intriguing observations, from
68 phylogenetically distant organisms, connecting G1/S transition regulators to multicellularity led us to
69 ask the following question. Could the evolution of the G1/S regulation pathway itself have somehow
70 favored multicellularity emergence and/or maintenance?

71 In this work we used *S. cerevisiae* to question the complex relationship between G1/S cell cycle
72 regulators and multicellularity. We took advantage of the snowflake model (14,15) in which
73 multicellularity is due to a genetic defect in cell separation caused by the deletion of Ace2, a
74 transcription factor that control the expression of chitinases and endoglucanases required for cell wall
75 degradation after cytokinesis completion (16,17). When planktonic *ACE2* and snowflake *ace2* cells
76 were co-cultured without applied selective pressure and their fitness compared, we observed that
77 *CLN3* deletion, as well as *WHI5* overexpression, favored the *ace2* snowflake form. We showed that exit
78 from quiescence is the critical stage leading to the *ace2 cln3* snowflakes selection. Importantly we

79 demonstrated that the *ace2* mutation, but not the snowflake phenotype, was responsible for the *cln3*
80 faster quiescence exit phenotype. Finally, we show that both the multicellularity and quiescence exit
81 phenotypes observed for *ace2* mutants are phenocopied by the *AMN1*^{368D} allele found in "non-
82 laboratory" yeast strains. Our results point to the possibility that evolution of cell cycle control could
83 promote the evolution of multicellularity as a passenger phenotype.

84

85 Results

86 The *ace2 cln3* snowflake strain is selected over the *ACE2 cln3* planktonic strain.

87 In order to investigate the relationship between the G1/S cell cycle regulators and multicellularity, we
88 used the yeast snowflake model in which the absence of Ace2, a transcription activator of several
89 chitinase and endoglucanases genes (18–20), results in the lack of separation of the daughter cell from
90 the mother cell after cytokinesis. It ensues that *ace2* mutant yeasts form cell clusters that grow and
91 end-up breaking most probably due to mechanical constraints (21). A major advantage of studying
92 snowflakes rather than inducible forms of multicellularity, such as pseudo-hyphae, is that unicellular
93 (planktonic, PK) and multicellular (snowflake, SF) yeast, differing only by one mutation in the *ACE2*
94 gene, can be co-cultivated and their fitness compared. We hence grew isogenic diploid *ACE2*/*ACE2* and
95 *ace2*/*ace2* cells of the BY (S288c-derived) background in minimal enriched medium (SD casa WAU).
96 Cultures of both genotypes were mixed to obtain a 50/50 ratio of *ace2* SF and *ACE2* PK strains, either
97 at the phenotype level (number of entities observed by microscopy, a SF being an entity with 4 or more
98 cells, Figure 1-figure supplement 1) or at the cell genotype level (by monitoring the *ace2::kanMX*
99 disruption using qPCR) (Figure 1A). The mixtures were then repeatedly grown to saturation and diluted
100 every 2 days, resulting in a total of more than 100 generations. Interestingly, the *ace2* strain showed
101 no selective advantage or disadvantage over the *ACE2* strain, both at the SF phenotype level (Figure
102 1B, black bars) and the genotype level (Figure 1C, black bars). This indicates that, under these growth

103 conditions, the *ace2* mutation and its multicellular phenotype have no effect on fitness. Strikingly,
104 when similar experiments were performed with *ace2* or *ACE2* strains carrying a deletion of the *CLN3*
105 gene, a deletion known to lengthen the G1 phase and to significantly increase cell volume (22), the
106 *ace2* snowflake strains rapidly took over the population (red bars, Figure 1B and 1C). A similar result
107 was obtained when *WHI5,* encoding the major downstream target of *CLN3*, was overexpressed (red
108 bars, Figure 1D). These results strongly suggest that the observed effect on population fitness takes
109 place through the *CLN3/WHI5* G1/S transition regulatory pathway. Together our results reveal a robust
110 phenotypic interaction between the G1/S transition major players, *CLN3* and *WHI5*, and the *ace2*
111 snowflakes.

112

113 *ace2 cln3* cells exit faster from quiescence than *ACE2 cln3*

114 In our competition experimental setup (Figure 1A), cultures alternate phases of active cell division with
115 stationary phases during which cells are in a quiescent state (Figure 2-figure supplement 1A).
116 Theoretically, the fitness advantage of the *ace2 cln3* strain over its *ACE2 cln3* isogenic counterpart
117 could be due to a faster doubling time during exponential growth, to a higher biomass yield of the
118 population, to a better survival in stationary phase or to a faster exit from stationary phase, each of
119 these possibilities (schematized Figure 2-figure supplement 1A) acting either alone or in combination.
120 We tested these four possibilities separately. First, we found that the population doubling times of the
121 two sets of strains was not significantly different (Figure 2-figure supplement 1B). In addition, *ace2* and
122 *ACE2* cell populations led to similar biomass accumulation indicating that the yield of carbon utilization
123 was not significantly modified by the *ace2* and/or the *CLN3* mutation (Figure 2-figure supplement 1C).
124 We then estimated cell survival in stationary phase by staining 2 days-old cells with methylene blue, a
125 dye that specifically accumulates in dead cells. No significant differences in dead cell percentages were
126 observed between *ace2* and *ACE2* cells should they be *cln3* or *CLN3* (Figure 2-figure supplement 1D).

127 From these experiments, we conclude that neither the doubling time, nor the biomass yield, or the cell
128 death rate could explain the selective advantage of the *ace2 cln3* cells over their *ACE2 cln3* counterpart.

129 We then compared the time required for *ace2 cln3* and *ACE2 cln3* quiescent-cell populations to exit
130 stationary phase. We found that the time required for population to resume proliferation after
131 refeeding, referred to as lag-time, was not significantly different between *ace2 CLN3* and *ACE2 CLN3*
132 cells (grey and black dots, Figure 2A). In addition, we confirmed that the lag-time was significantly
133 longer for the *ACE2 cln3* (light red dots) than for *ACE2 CLN3* cell population (black dots) (Figure 2A), as
134 previously described (23,24). Indeed, after refeeding of stationary phase cultures, *CLN3* transcription
135 is increased by 5- to 10-fold within five minutes (24). Cln3 is hence likely to play an important role for
136 quiescent cells to move out from G1 and reenter proliferation. Importantly, this difference was
137 partially but significantly suppressed in *ace2 cln3* (red dots) cell populations (Figure 2A) suggesting that
138 the *ace2* mutation genetically suppresses the *cln3* strain lag-time defect. We then re-fed quiescent
139 cells on microscope agarose pads containing new medium and addressed cell ability to emit a new bud
140 *i.e.* to exit quiescence. While the time required by cells to exit quiescence was not significantly different
141 between *ace2 CLN3* and *ACE2 CLN3* strains (Figure 2-figure supplement 1E), it was significantly lower
142 for the *ace2 cln3* cells than for the *ACE2 cln3* cells (Figure 2C). Importantly, similar observations were
143 made with haploid *ace2 cln3* cells (Figure 2D) for which snowflakes are much smaller (Figure 2-figure
144 supplement 1G-K). Indeed, not only haploid cells display a smaller cell volume than diploid cells, but
145 their proximal budding pattern make haploid snowflakes much more globular than diploid snowflakes
146 that are rather elongated (25). This observation confirmed the robustness of the *cln3* phenotype and
147 its suppression by *ace2*. It also suggests that this phenotype is not dependent on the size of the
148 snowflake entity. Altogether these results point to quiescence exit as the key step accounting for the
149 competition outcomes.

150 A simple prediction from these results is that a competition experiment in co-culture ran under
151 conditions where the cells are always maintained in proliferation should not result in any fitness

152 difference between for *ace2 cln3* and *ACE2 cln3* cells. This is what was observed when maintaining
153 these two strains in proliferation for 94hrs (corresponding to at least 70 generations, Figure 2E, left
154 panel), by contrast to an equivalent number of generations obtained by alternating proliferation and
155 stationary phases (Figure 2E, right panel). Reciprocally, as described previously (26), increasing the
156 duration of stationary phase caused an increase of the lag phase length at the population level (Figure
157 2F). Importantly, it also increased the fitness advantage of *ace2 cln3* over *ACE2 cln3* cells (red and pink
158 bars Figure 2G), while there was still no difference between *ace2 CLN3* and *ACE2 CLN3* cells (black and
159 grey bars Figure 2G). Altogether, our results pinpoint exit from quiescence as the critical stage in which
160 the *ace2 cln3* snowflakes are positively selected.

161

162 The advantage of *ace2 cln3* during quiescence exit is independent of the 163 snowflake phenotype

164 Why do *ace2 cln3* cells exit quiescence faster than *ACE2 cln3* cells? This could be due to some specificity
165 associated with *cln3* mutation that would modify the snowflake properties. Alternatively, it could be
166 dependent on the specific *ace2 cln3* mutation combination independently of the snowflake
167 phenotype. To answer this question, we dissociated the snowflake phenotype from the *ace2* mutation
168 and vice versa.

169 First, we asked whether the snowflake phenotype was sufficient, independently of the *ace2* mutation,
170 to rescue the quiescence-exit default associated with *cln3*. Ace2 is a transcription factor that induces
171 the expression of several chitinases and endoglucanases necessary for the septum digestion and cell
172 separation. To mimic the *ace2* snowflake phenotype, we constructed a quintuple chitinase and
173 endoglucanase mutant (*cts1, dse2 dse4, egt2, scw11*), hereafter "quintuple mutant", that results in a
174 snowflake phenotype comparable to that of the *ace2* mutant (Figure 3-figure supplement 1) while
175 carrying the wild-type *ACE2* allele. When combined with the *cln3* mutation, the five deletions have no

176 effect on quiescence exit efficiency (Figure 3A). Accordingly, the *cln3 ace2* strain exited quiescence
177 much more efficiently than the *cln3* quintuple mutant (Figure 3B). This indicates that the *ace2* mutation
178 itself, and not multicellularity, suppresses the quiescence exit defect of the *cln3* mutant. Finally,
179 competition experiments in co-cultures initially containing equal proportion of quintuple mutant and
180 WT cells confirmed that the snowflake phenotype is not sufficient to give the *cln3* mutant a
181 phenotypical advantage (Figure 3C).

182 Reciprocally, we asked whether the *ace2* mutation itself, independently of the snowflake phenotype,
183 could be sufficient to rescue the quiescence-exit default associated with *cln3*. We thus examined
184 whether planktonic cells obtained in an *ace2* mutant background would still behave as their snowflake
185 counterparts. To obtain planktonic *ace2* cells, we used sonication to physically break the snowflakes,
186 before triggering quiescence exit. Mild sonication resulted in an increased proportion of planktonic
187 cells in the *ace2 cln3* cell population (up to 50%, Figure 4-figure supplement 1A) with no defect in cell
188 survival (Figure 4-figure supplement 1B). After sonication, isolated cells, small and large cell clusters
189 displayed a similar quiescence exit efficiency (Figure 4A). Furthermore, the sonicated and non-
190 sonicated cells had the same quiescence exit efficiency, indicating that sonication *per se* had no
191 significant impact (Figure 4-figure supplement 1C). Still, after sonication, *cln3 ace2* isolated cells exited
192 quiescence faster than their *cln3 ACE2* counterpart (Figure 4B). These results show that the snowflake
193 phenotype is not necessary for the ability of the *ace2 cln3* mutant to exit quiescence faster than *ACE2*
194 *cln3* cells.

195 Together, our results with the haploid strains, the quintuple mutant and sonication experiments
196 establish that the *ace2* mutation, but not the snowflake phenotype, is responsible for the *cln3* fast
197 quiescence exit phenotype.

198

199 **The *ace2 cln3* fast quiescence exit phenotype is dependent on the Kss1 MAP**
200 **kinase**

201 As previously mentioned, a delay of *cln3* mutants to exit quiescence was already documented (24).
202 Why is this phenotype suppressed by the *ace2* deletion? Among Ace2 well-established targets , *AMN1*,
203 *BUD9, CHS7, CTS1, DSE2, DSE4* and *SCW11* are activated, while *KSS1* is down regulated by Ace2 (18).
204 Four of those, namely *CTS1, DSE2, DSE4* and *SCW11*, are not involved in suppressing the delay
205 phenotype since they are mutated in the quintuple mutant that, in combination with *cln3*, has the
206 same delay as a single *cln3* mutant (Figure 3D). We focused on Kss1, a MAP kinase involved in
207 filamentous growth and mating (27,28), because the Kss1 pathway was previously found to positively
208 regulate *CLN1,* a G1 cyclin encoding gene that is partially redundant to *CLN3* (29). We hypothesize that
209 deletion of *ACE2* would result in higher *KSS1* expression (18) that in turn, could lead to higher *CLN1*
210 expression and thereby be responsible for the *cln3* mutation suppression. We hence tested whether
211 suppression of *cln3* by *ace2* was dependent on *KSS1* by comparing quiescence exit efficiency of *ace2*
212 *cln3 KSS1* and *ace2 cln3 kss1* cells. Clearly, the knock-out of *KSS1* totally abolished the phenotypic
213 suppression of *cln3* by *ace2* (Figure 5A). Further, *CLN1* expression upon quiescence exit was
214 significantly higher in the *ace2 cln3* than in the *ACE2 cln3* strain (Figure 5B), this difference of
215 expression being entirely abolished in the absence of *KSS1* (Figure 5C). We conclude that the
216 competitive advantage of the *ace2* mutant over its *ACE2* wild-type counterpart is most likely due to
217 higher expression of *CLN1* that, at least partially, compensates for the absence of *CLN3*. Importantly,
218 this transcriptional effect of Ace2 on *CLN1*, *via* Kss1, is independent of the role of Ace2 on
219 multicellularity.

220

221 **The *AMN1*^{368D} allelic-form found in the wild, phenocopies the *ace2* deletion**

222 In laboratory strains, the Ace2 protein level is constant throughout the cell cycle, while it is not always
223 the case in non-laboratory strains (25). This is due to the presence of the recessive *amn1*^{368V} allelic
224 form in laboratory strains (hereafter *amn1-368V*), which was probably initially selected to avoid
225 "unwanted" cell clusters. In non-laboratory strains, the Amn1-368D protein induces the proteolysis of
226 Ace2 through the ubiquitin proteasome pathway (25). It thus appears that the Amn1/Ace2 tandem has
227 an important physiological role associated with optional post-mitotic cell separation. We first observed
228 that expression of *AMN1*^{368D} in the BY background resulted in a snowflake phenotype comparable to
229 that of *ace2* mutant strains (Figure 6-figure supplement 1). We then asked whether *AMN1*^{368D} allelic
230 form could suppress the quiescence exit delay of the *cln3* mutant. Indeed, the *cln3 AMN1*^{368D} strain
231 exited quiescence much more rapidly than the *cln3 amn1-368V* strain (Figure 6A). Finally, we found
232 that the *AMN1*^{368D} strain was strongly enriched in competition experiments when associated with a
233 *cln3* mutation (Figure 6B) or with *WHI5* overexpression (Figure 6C). We conclude that, in haploid yeast,
234 the *AMN1*^{368D} allelic-form phenocopies both the multicellularity and the suppression phenotypes of
235 the *ace2* mutant.

236

237 # Discussion

238 In this work, we took advantage of the snowflake model of multicellularity that is genetically
239 determined, by *ace2* or *AMN1* and is hence not triggered by external cues, as it is often the case for
240 facultative multicellularity. This experimental design allows direct fitness measurements between uni-
241 and multicellular entities. Importantly, in a wild-type background, multicellularity was neither selected
242 nor counter-selected, even following a substantial period of co-culture. This establishes that simple
243 multicellular cluster formation should not always come at a cost, contrary to the general assumption
244 in the literature (30,31). Such a neutral effect of multicellularity on fitness could easily result in
245 phenotypical *aller-retours* between unicellularity and multicellularity during evolution. In fact, such
246 *aller-retours* are observed during the life cycle of non-laboratory strains in which diploids are

247 planktonic while haploid strains form clusters (32). Here we show that the evolution of the cell cycle
248 regulation may interact with the multicellular phenotype. We revealed a genetic connection between
249 major G1/S regulators and *AMN1* and *ACE2*, key actors modulating cell cohesion at the end of mitosis
250 (Figure 7). Interestingly, this connection operates differently in laboratory strains carrying the *amn1-*
251 *368V* allele (Figure 7A) and strains carrying the $AMN1^{368D}$ allele (Figure 7B). We established that this
252 genetic interaction is due to the pleiotropy of the *ace2* mutation, affecting not only the chitinases and
253 endoglucanases that are critical for septum digestion and cell separation, but also the Kss1 MAP kinase
254 which contributes to the activation of Cln1, one of the G1 cyclins. This phenotypical link between *CLN1*
255 expression and multicellularity, achieved by Ace2 function, is particularly important during quiescence
256 exit, a situation that is likely to happen very often under ecological conditions, such as boom and bust
257 cycles when moving from rotting fruit to rotting fruit. We propose that in some instances,
258 multicellularity may have evolved as a side effect, named here "passenger phenotype", of another
259 phenotype that was the one selected (Figure 7B). Since transcription factors often have multiple
260 targets, an alteration in their expression or function leading to the selection of a phenotype due to one
261 of the targets could easily lead to the selection of additional phenotypes due to other targets. This
262 could be a common feature involved in evolutionary processes.

263 Connections between G1/S regulators and multicellularity have been repeatedly observed in
264 phylogenetically distant species (see introduction section), suggesting a propitious genetic interplay
265 for co-evolution. Olson and co-workers have shown that RB could have played a role in early steps of
266 multicellularity evolution *via* a cooption mechanism favoring the appearance of simple multicellular
267 entities (9). Our work further supports a role for G1/S regulators in evolution of multicellularity, but
268 the mechanism appears different and affects selection of multicellularity rather than its initial
269 appearance. We show that the *ace2* or $AMN1^{368D}$ allelic forms are sufficient to counteract a negative
270 fitness effect of the overexpression of the RB functional orthologue Whi5 (Figure 1D, Figure 6F).
271 Importantly we have shown that this phenotypic suppression is independent of the multicellular
272 phenotype associated with the *ace2* or $AMN1^{368D}$ allelic forms. This observation led us to propose that

273 some regulatory effects on the G1/S transition could be alleviated by Amn1 degradation of Ace2 and
274 thereby connected to multicellularity. In this hypothesis the selective pressure applies on G1/S
275 transition efficiency and not on multicellularity itself. It is hence different from the cooption hypothesis
276 in which the RB protein acquired new functionalities leading to multicellularity that would result in
277 some directly selectable fitness advantage. Both scenarios imply co-evolution of cell cycle regulation
278 and multicellularity, which could therefore be a much more general feature than first thought. It could
279 indeed be a case of convergent evolution as suggested by the fact that it may involve distinct
280 mechanisms.

281 More generally, our results prompted us to reconsider whether simple multicellularity, which
282 appeared multiple times in evolution, was always selected for the new physical and physiological
283 properties it provides (2). Alternatively, it is possible that multicellularity was initially selected as a
284 byproduct, allowing it to be maintained although not necessarily increasing fitness as such. This would
285 contribute to disconnect the initial selection of simple multicellularity from the selection of further
286 associated advantages, such as division of labor, that would require time and necessitate that the
287 multicellularity phenotype would not be counter-selected in the first place. Such a passenger selection
288 of multicellularity would make it independent of physical constraints such as size or shape that could
289 restrain its further evolution. The work presented here provides a proof of concept that such a scenario
290 is plausible and may have contributed to the multiple appearance of multicellularity in the tree of life.

291

292 # Materials and methods

293

294 ## Yeast media and strains, plasmids and oligonucleotides

295 Yeast cells were grown in liquid or solid media at 30 °C. SD is a synthetic minimal medium containing
296 0.5% ammonium sulfate, 0.67% yeast nitrogen base (Difco), 2% glucose. SDcasaWAU is an SD medium

297 supplemented with 0.2% casamino acids (Difco) tryptophan (0.2 mM), adenine (0.3 mM) and uracil
298 (0.3 mM). Unless specified, cells were grown in SDCasaWAU medium. When indicated, medium was
299 depleted in uracil, resulting in a medium named SDCasaWA, allowing the selection of cells expressing
300 a vector carrying *URA3* marker. SC medium was prepared as described by Sherman (33) and was
301 supplemented by histidine (0.06 mM), leucine (0.5 mM), lysine (0.07 mM), tryptophan (0.2 mM),
302 adenine (0.3 mM), and uracil (0.3 mM). The medium obtained by the depletion of both uracil and
303 leucine, called SC-U-L medium, allows the selection of cells expressing both *URA3* and *LEU2* markers.
304 The YPD medium contained 1% yeast extract, 2% peptone, and 2% glucose.

305 Yeast strains (listed in Table 1) are derived from both FY4 and FY5 prototrophic strains and from
306 disrupted strains isogenic to BY4741 or BY4742 purchased from Euroscarf (Frankfurt, Germany). Strains
307 described in Table 1 were either obtained by crossing, sporulation, and micromanipulation of meiosis
308 progeny or by transformation of cells with a DNA fragment of interest (plasmid, PCR product). Yeast
309 strains were transformed using the lithium acetate method (34).

310 **Table 1: Strains**

Strain name	Genotype
FY4	
Y12580, Y12581, Y12582	*cln3::URA3/cln3::URA3 ura3Δ0/ura3Δ0 leu2Δ0/leu2Δ0*
Y12584, Y12585, Y12586	*ace2::KanMX4/ace2::KanMX4 cln3::URA3/cln3::URA3 ura3Δ0/ura3Δ0 leu2Δ0/leu2Δ0*
Y12606, Y12607, Y12608	*leu2Δ0/leu2Δ0*
Y12973, Y12974, Y12975	*ace2::KanMX4/ace2::KanMX4 leu2Δ0/leu2Δ0*
Y12575 + p5314	*ace2::KanMX4/ace2::KanMX4 ura3Δ0/ura3Δ0* carrying empty plasmid 2µ
(Y11418xY12599) + p5314	*ura3Δ0/ura3Δ0* carrying empty plasmid 2µ
Y12575 + p4726	*ace2::KanMX4/ace2::KanMX4 ura3Δ0/ura3Δ0* carrying plasmid 2µ *WHI5*
(Y11418xY12599) + p4726	*ura3Δ0/ura3Δ0* carrying plasmid 2µ *WHI5*
Y12512	*ace2::KanMX4/ace2::KanMX4 HTB1-3xCFP-LEU2/HTB1-3xCFP-LEU2 ura3Δ0/ura3Δ0 his3Δ1/HIS3*
Y12565, Y12566, Y12958	*ace2::KanMX4 cln3::URA3 ura3Δ0 leu2Δ0*
Y12567, Y12568, Y12959	*cln3::URA3 ura3Δ0 leu2Δ0*

Y12408, Y12595, Y12596	*ace2::KanMX4 leu2Δ0*
Y11417, Y12571	*leu2Δ0*
Y12709, Y12710, Y12711	*cln3::URA3/cln3::URA3 ura3Δ0/ura3Δ0 leu2Δ0/leu2Δ0*
Y12716, Y12717, Y12718	*dse2::KanMX4/dse2::KanMX4 cts1::KanMX4/cts1::KanMX4 scw11::KanMX4/scw11::KanMX4 egt2::KanMX4/egt2::KanMX4 dse4::KanMX4/dse4::KanMX4 cln3::URA3/cln3::URA3 ura3Δ0/ura3Δ0 leu2Δ0/leu2Δ0*
Y12976, Y12977, Y12978	*dse2::KanMX4/dse2::KanMX4 cts1::KanMX4/cts1::KanMX4 scw11::KanMX4/scw11::KanMX4 egt2::KanMX4/egt2::KanMX4 dse4::KanMX4/dse4::KanMX4 leu2Δ0/leu2Δ0*
Y12967, Y12968	*kss1::KanMX4 ace2::KanMX4 cln3::URA3 ura3Δ0 leu2Δ0*
Y12969, Y12970	*kss1::KanMX4 cln3::URA3 ura3Δ0 leu2Δ0*
Y12838, Y12839, Y12840	*AMN1368D-URA3-AMN1368V ura3Δ0 leu2Δ0*
Y12935, Y12936, Y12937	*AMN1368V-URA3-AMN1368V ura3Δ0 leu2Δ0*
Y12942, Y12943, Y12944	*AMN1368D-URA3-AMN1368V cln3::KanR ura3Δ0 leu2Δ0 his3Δ1*
Y12946, Y12947, Y12949	*AMN1368V-URA3-AMN1368V cln3::KanR ura3Δ0 leu2Δ0 his3Δ1*
Y12838 + p338	*AMN1368D-URA3-AMN1368V ura3Δ0 leu2Δ0* carrying empty plasmid 2µ
Y12935 + p6053	*AMN1368D-URA3-AMN1368V ura3Δ0 leu2Δ0* carrying plasmid 2µ *WHI5*
Y12838 + p338	*AMN1368D-URA3-AMN1368V ura3Δ0 leu2Δ0* carrying empty plasmid 2µ
Y12935 + p6053	*AMN1368D-URA3-AMN1368V ura3Δ0 leu2Δ0* carrying plasmid 2µ *WHI5*
GN-1C	*HO:NatR AMN1368D FLO8+*

All plasmids and oligonucleotides are listed in Table 2 and Table 3, respectively. To construct the plasmids allowing the overexpression of *WHI5* in yeast strains, the open reading frame of the *WHI5* gene, driven by its own promoter, was amplified using the genomic DNA of the FY4 strain as a template. The PCR product was then cloned into two 2µ vectors, YEpLac195 and YEpLac181, carrying respectively *URA3* and *LEU2* markers. Two plasmids carrying respectively two different alleles of the *AMN1* gene were also constructed. The open reading frame of the *AMN1* gene was amplified using either the FY4 strain genomic DNA (*amn1*^{368V} PCR product) or the GN-1C strain genomic DNA (*AMN1*^{368D} PCR product). The GN-1C strain was a generous gift from Pr. Marullo. The PCR products were cloned into YIpLac211, that allowed integration of the cloned *AMN1* allele at the yeast *AMN1* locus.

321 **S2 Table: Plasmids**

Plasmid Name	Description	
p5314	YEpLac195: 2µ *URA3* AmpR	(35)
p4726	*WHI5* in YEpLac195	lab collection
p338	YEpLac181 : 2µ *LEU2* AmpR	(35)
p6053	*WHI5* in YEpLac181	This study
p6164	YIpLac211 : integrative plasmid *URA3* AmpR	(35)
p6165	*AMN1-368D* in YIpLac211	This study
p6167	*AMN1-368V* in YIpLac211	This study

322

323 **S3 Table: Oligonucleotides**

Oligonucleotide name	Sequence 5'-3'
qPCR locus ACE2 -26 forward	GGACCAAAAACGGTGTTAATACAATC
qPCR KanMX4 specific reverse	CTGGCGCGCCTTAATTAACC
qPCR ACT1 forward (coding)	CCCCAGAAGAACACCCTGTTC
qPCR ACT1 reverse (coding)	CGTAGAAGGCTGGAACGTTG
qPCR CLN1 coding forward	ATCGATCAGCAACCGGAGAT
qPCR CLN1 coding reverse	AACCTGACAGCGTGGAAGAA
KanB reverse	CTGCAGCGAGGAGCCGTAAT
ACE2 promoter forward	CGTCACTCCATTAGAATCCC
CLN3 promoter forward	TCCTCATTCGGTTTAACTCC
CLN3 terminator reverse	TGACTAGAGGAAGTAAGGAG
DSE2 promoter forward	CAGTAGAGCTAACCACAGTC
CTS1 promoter forward	ACTGTCGCTCGTTTCACAAC
SCW11 promoter forward	CAGTTACGCAACAAAGACAG
DSE4 promoter forward	ACTACAAGCGAGGGTAAAGG
EGT2 promoter forward	GATGCTGGTTTGATGCTAAG
CLN3 promoter -500 forward	TGAGGAAAGAGGACTATACC
CLN3 terminator +500 reverse	TAGGTAGCGATGAAGATTGG
URA3 promoter -500 forward	TCATCATCTCATGGATCTGC
URA3 terminator +500 reverse	TACGCCAGTACACCTTATCG
CLN1 promoter -200 forward	CCAAGGAGTTCTTCGTTCGC
CLN1 terminator +200 reverse	TCGCGTCATCTTTTCCGTTC
AMN1 promoter -75 forward	GTTTAATATCCATCCATTCC
AMN1 +459 forward	CCTTTGACTGCTCAACATCAG
AMN1 +882 forward	CATCAAGTAACACAACCAG
AMN1 +1269 forward	GGTTGTGATGTTGATGATG
AMN1 terminator +169 reverse	GTTTCTTCGGCCCTTCTGGA
AMN1 +1269 reverse	CATCATCAACATCACAACC

AMN1 +882 reverse	CTGGTTGTGTTACTTGATG
AMN1 +376 reverse	GAAAGACTGGATGCAGAAAC
Mat a and alpha forward	AGTCACATCAAGATCGTTTATGG
Mat a specific reverse	CTCCACTTCAAGTAAGAGTTTG
Mat alpha specific reverse	GCACGGAATATGGGACTACTTCG
WHI5 BamHI forward	CGCGGATCCCAAATCGGATATGAGCAGCTG
WHI5 PstI reverse	ACGTCTGCAGGCTCGAGGCGATCTGTCGC
M13 reverse	CAGGAAACAGCTATGACC
AMN1 BamHI forward	GTTGGATCCATGAAACTAGAACGCG
AMN1 PstI reverse	AACCTGCAGCTAGTCCACATTATTCTCTATTTCG

Description of a Snowflake population

Snowflake populations or co-culture between Snowflake and Planktonic strains were observed in a Kova Glasstic slide (Kova international, 87144F). The proportion of the Snowflake phenotype in these populations was determined by counting entities formed by four or more cells. To characterize the size of Snowflakes within a population, the population was observed between slide and coverslip separated by a layer of double-sided adhesive tape. The longest segment of the Snowflake entity was measured, as well as the longest segment perpendicular to the first segment and lying in the same Z plane.

Competitions experiment in co-culture

Snowflake strains (either *ace2* or quintuple mutant or *AMN1*^{368D}) and planktonic strains were grown in monocultures to stationary phase, for 2 days unless specified. Snowflake and planktonic strains were then mixed in indicated proportion and co-cultured. Unless specified, every 2 days, co-cultures, after they reached stationary phase, were diluted by a factor of 1000 into fresh liquid medium (10µl in 10ml).

To set up the co-cultures for which the proportion of Snowflake phenotype was monitored, the entity (Snowflake entity or single-cell entity) concentrations in each of the monocultures were determined. The volumes of the 2 monocultures in the mix were accordingly determined and then adjusted to

341 obtain 50% of Snowflake entity in the mix. The proportion of Snowflakes in the co-culture was
342 determined every two days before dilution in fresh medium.

343 To set up the co-cultures for which the proportion of *ace2* genotype was monitored, the two strains
344 were mixed to obtain a 50/50 cell ratio. Every 2 days, the genomic DNA of the stationary phase co-
345 cultures was extracted by phenol-chloroform protocol. Quantitative PCR amplifications were then
346 performed with GoTaq® qPCR Master Mix (Promega, A6001), using 50ng of DNA extracted from co-
347 cultures. The first set of primers was designed to amplify the *ace2::KanMX4* locus with the first primer
348 targeting the region directly upstream of the ATG of the *ACE2* gene, and the second primer targeting
349 a region specific to the *KanMX4* marker (Supplemental Table 3). The second set of primers targeted a
350 region of *ACT1* gene (Supplemental Table 3).

351 For competitions in which the co-cultures were maintained in proliferation phase for 94 hours, the co-
352 cultures were diluted every 8 hours to ensure that the OD_{600nm} was always maintained below 0.5.

353

354 Population measurement

355 To determine the population doubling time of yeast strains, cells were kept in exponential proliferation
356 phase ($OD_{600nm} \leq 1.0$) for at least 24 hours by successive dilutions before any measurement. Population
357 doubling time was then determined by following the optical density at 600 nm during 5 hours on at
358 least three independent exponential growth culture. Population doubling time was then determined
359 by exponential growth regression of the proliferation curves using GraphPad Prism 8 (GraphPad
360 Software, Inc. La Jolla, USA).

361 To determine cell viability, the cells were stained with a solution containing 0.2% of methylene blue
362 (Sigma-Aldrich, Saint Louis, MI, USA) and 2% sodium citrate pH7. After 5 minutes of incubation, the
363 proportion of blue-stained dead cells was scored manually.

364 The biomass yield of cultures was determined by filtration of 2-day stationary phase cultures on 0.45
365 µm polyamide pre-weighted filters (25006–47-N; Sartorius). The filter was washed twice with 10 mL of
366 miliQ water and then dried with successive 30 seconds cycles in a microwave oven at 800 W until the
367 mass of the filter and cells was constant.

368 Cell volume was measured by microscopy using the spheroid formula: $4/3*\pi*a^2*c$, where a and c are
369 the equatorial and polar radius respectively.

370

371 Refeeding of stationary phase cultures

372 Unless the age of cultures is otherwise specified, 2-day stationary phase liquid monocultures were
373 refed either on liquid or solid fresh SDcasaWAU medium.

374 Stationary phase cultures were refed by dilution into liquid fresh SDcasaWAU medium at
375 approximately 0.05 OD_{600nm}. The OD_{600nm} was monitored upon refeeding for at least 7 hours covering
376 both 'lag' and exponential phases (until at least a 5-fold increase of the OD_{600nm} compared to the initial
377 point). To quantify the duration of the 'lag' phase, we normalized all the OD_{600nm} values of each
378 individual growth curve to their respective initial OD_{600nm} value and then applied the logarithmic
379 function to all the normalized OD_{600nm} values of the growth curve. We next performed a linear
380 regression on the points corresponding to the proliferation phase of the growth curve using GraphPad
381 Prism 8 (GraphPad Software, Inc. La Jolla, USA). The time value for which the linear regression
382 intersects the Time-X axis corresponds to the end of the 'lag' phase and the beginning of the
383 proliferation phase, and is referred as 'the duration of lag phase'.

384 Quiescent cells from stationary phase cultures were also refed onto solid medium. Cells were spread
385 onto half a 3% agarose microscope pad made of fresh SDcasaWAU. Bright field images of individual
386 cells were then captured every 15 minutes for up to 4 hours. The cells forming an unequivocal new
387 bud upon refeeding were scored.

388 When indicated, an aliquot of stationary phase culture can be sonicated before a refeeding experiment
389 on microscope agarose pad. Cycles of 30 seconds in a sonication bath were carried out until the
390 proportion of single-cell entities in the *ace2* SF culture increased to a desired proportion
391 (approximately 40%).

392

393 Determination of *CLN1* mRNA level upon refeeding by Reverse transcriptase-
394 PCR.

395 To determine the level of *CLN1* mRNA upon refeeding of 2-day stationary phase cultures, 15 mL of a
396 2-day culture was diluted in 85 mL of fresh medium. Fifteen minutes upon refeeding, 25 mL of culture
397 was sampled and centrifuged at 4000 rpm at 4°C for 3 min. The pellet was washed in 1 mL of RNase-
398 free H2O, and centrifuged at 12,000 g at 4°C for 30 seconds. A Tri-Reagent (Sigma, T9424) protocol
399 was then performed to extract total RNA. A reverse-transcription of 200ng of total RNA using the 'High
400 Capacity cDNA Reverse Transcription' Kit (ThermoFisher, 4368813) was then performed. The cDNA was
401 diluted to 1/25 and amplified with a Quantitative-PCR protocol, using the GoTaq® qPCR Master Mix
402 (Promega, A6001) and primers specific to the coding region of *CLN1* or the coding region of *ACT1*
403 (Supplemental Table 3).

404

405 Microscopy

406 The refeeding experiments on microscope pad, as well as the Snowflake size-measurement
407 experiments were carried out using a Zeiss 200M inverted microscope (Carl Zeiss, Thornwood, NY,
408 USA) with the additional equipment : a MS-2000 stage (Applied Scientific Instrumentation, Eugene,
409 OR, USA), a Lambda LS 300 W xenon light source (Sutter, Novato, CA, USA), a 5 positions filter turret, a
410 100X 1.4NA Plan-Apochromat objective and a CoolSnap HQ camera (Roper Scientific, Tucson, AZ, USA).

411 The filters are from Chroma Technology Corp. The microscope and additional equipment were
412 controlled by SlideBook software 5.0. (Intelligent Imaging Innovations, Denver, CO, USA). The images
413 were analyzed with Image J. All other microscopy experiments were carried out using Zeiss Primo Star
414 microscope, equipped with a 40X/0.65 Plan-Achromat objective.

415

416 **Statistical analysis**

417 All experiments were carried out at least three times on independent biological samples. The exact
418 number of independent samples is indicated in the figure legends. Data are presented as mean ± SD.
419 All the statistical analyses were done using GraphPad Prism 8 (GraphPad Software, Inc. La Jolla, USA).
420 The proportion of SF in competition experiments, the refeeding experiments on microscope pad and
421 the proportion of dead cells were analyzed by Fisher's exact test on a contingency table. Other
422 experiments are analyzed by Welch's unpaired t-test. p-values below 0.05 are represented by *; p
423 values inferior to 0.005 are represented by **; and p values inferior to 0.001 are represented by ***.
424 p-values superior to 0.05 were considered non-significant and are represented by 'ns'.

425

426 # Acknowledgments and funding sources

427 The authors thank Benoît Pinson for technical advising, the members of the Sagot lab for discussions
428 on the project and Isabelle Sagot for critical reading of the manuscript. The authors also thank Sabine
429 Vaur for her help with the qPCR method. This work was supported by a grant from Ligue Régionale
430 Contre le Cancer (2022 Dordogne) to BD-F. TD was supported by a grant from University of Bordeaux,
431 NewMoon RRI Program on Cancer in Evolution.

432

433 # Author contributions

T.L.D., D.L. and B.D.-F. designed research; T.L.D. performed research; T.L.D., D.L. and B.D.-F. analyzed data; and T.L.D. and B.D.-F. wrote the paper.

Competing interests

The authors declare no competing interest.

References

1. Grosberg RK, Strathmann RR. The Evolution of Multicellularity: A Minor Major Transition? Annu Rev Ecol Evol Syst. 1 déc 2007;38(1):621-54. doi:10.1146/annurev.ecolsys.36.102403.114735

2. Tong K, Bozdag GO, Ratcliff WC. Selective drivers of simple multicellularity. Current Opinion in Microbiology. juin 2022;67:102141. doi:10.1016/j.mib.2022.102141

3. La Fortezza M, Schaal K, Velicer GJ. Why Aggregate? On the Evolution of Aggregative Multicellularity [Internet]. 2021 [cité 28 avr 2025]. Disponible sur: https://www.preprints.org/manuscript/202105.0451/v1 doi:10.20944/preprints202105.0451.v1

4. Newell PC, Telser A, Sussman M. Alternative Developmental Pathways Determined by Environmental Conditions in the Cellular Slime Mold *Dictyostelium discoideum*. J Bacteriol. nov 1969;100(2):763-8. doi:10.1128/jb.100.2.763-768.1969

5. Gimeno CJ, Ljungdahl PO, Styles CA, Fink GR. Unipolar cell divisions in the yeast S. cerevisiae lead to filamentous growth: Regulation by starvation and RAS. Cell. mars 1992;68(6):1077-90. doi:10.1016/0092-8674(92)90079-R

6. Kumar A. The Complex Genetic Basis and Multilayered Regulatory Control of Yeast Pseudohyphal Growth. Annu Rev Genet. 23 nov 2021;55(1):1-21. doi:10.1146/annurev-genet-071719-020249

7. Daignan-Fornier B, Laporte D, Sagot I. Quiescence Through the Prism of Evolution. Front Cell Dev Biol. 29 oct 2021;9:745069. doi:10.3389/fcell.2021.745069

8. Bertoli C, Skotheim JM, De Bruin RAM. Control of cell cycle transcription during G1 and S phases. Nat Rev Mol Cell Biol. août 2013;14(8):518-28. doi:10.1038/nrm3629

9. Hanschen ER, Marriage TN, Ferris PJ, Hamaji T, Toyoda A, Fujiyama A, et al. The Gonium pectorale genome demonstrates co-option of cell cycle regulation during the evolution of multicellularity. Nat Commun. 22 avr 2016;7(1):11370. doi:10.1038/ncomms11370

10. MacWilliams H, Doquang K, Pedrola R, Dollman G, Grassi D, Peis T, et al. A retinoblastoma ortholog controls stalk/spore preference in *Dictyostelium*. Development. 1 avr 2006;133(7):1287-97. doi:10.1242/dev.02287

11. Bachewich C, Whiteway M. Cyclin Cln3p Links G_1 Progression to Hyphal and Pseudohyphal Development in *Candida albicans*. Eukaryot Cell. janv 2005;4(1):95-102. doi:10.1128/EC.4.1.95-102.2005

12. Loeb JDJ, Kerentseva TA, Pan T, Sepulveda-Becerra M, Liu H. Saccharomyces cerevisiae G1 Cyclins Are Differentially Involved in Invasive and Pseudohyphal Growth Independent of the Filamentation Mitogen-Activated Protein Kinase Pathway. Genetics. 1 déc 1999;153(4):1535-46. doi:10.1093/genetics/153.4.1535

13. Cross FR, Buchler NE, Skotheim JM. Evolution of networks and sequences in eukaryotic cell cycle control. Phil Trans R Soc B. 27 déc 2011;366(1584):3532-44. doi:10.1098/rstb.2011.0078

475 14. Ratcliff WC, Pentz JT, Travisano M. TEMPO AND MODE OF MULTICELLULAR ADAPTATION IN
476 EXPERIMENTALLY EVOLVED *SACCHAROMYCES CEREVISIAE*. Evolution. juin 2013;67(6):1573-81.
477 doi:10.1111/evo.12101

478 15. Ratcliff WC, Denison RF, Borrello M, Travisano M. Experimental evolution of multicellularity. Proc
479 Natl Acad Sci U S A. 31 janv 2012;109(5):1595-600. doi:10.1073/pnas.1115323109 PubMed
480 PMID: 22307617; PubMed Central PMCID: PMC3277146.

481 16. Ratcliff WC, Fankhauser JD, Rogers DW, Greig D, Travisano M. Origins of multicellular evolvability
482 in snowflake yeast. Nat Commun. mai 2015;6(1):6102. doi:10.1038/ncomms7102

483 17. Koschwanez JH, Foster KR, Murray AW. Improved use of a public good selects for the evolution
484 of undifferentiated multicellularity. eLife. 2 avr 2013;2:e00367. doi:10.7554/eLife.00367

485 18. Mostovoy Y, Thiemicke A, Hsu TY, Brem RB. The Role of Transcription Factors at Antisense-
486 Expressing Gene Pairs in Yeast. Genome Biol Evol. juin 2016;8(6):1748-61.
487 doi:10.1093/gbe/evw104

488 19. Voth WP, Olsen AE, Sbia M, Freedman KH, Stillman DJ. *ACE2* , *CBK1* , and *BUD4* in Budding and
489 Cell Separation. Eukaryot Cell. juin 2005;4(6):1018-28. doi:10.1128/EC.4.6.1018-1028.2005

490 20. Doolin M, Johnson AL, Johnston LH, Butler G. Overlapping and distinct roles of the duplicated
491 yeast transcription factors Ace2p and Swi5p. Molecular Microbiology. avr 2001;40(2):422-32.
492 doi:10.1046/j.1365-2958.2001.02388.x

493 21. Jacobeen S, Pentz JT, Graba EC, Brandys CG, Ratcliff WC, Yunker PJ. Cellular packing, mechanical
494 stress and the evolution of multicellularity. Nature Phys. mars 2018;14(3):286-90.
495 doi:10.1038/s41567-017-0002-y

496 22. Nash R, Tokiwa G, Anand S, Erickson K, Futcher AB. The WHI1+ gene of Saccharomyces cerevisiae
497 tethers cell division to cell size and is a cyclin homolog. The EMBO Journal. déc
498 1988;7(13):4335-46. doi:10.1002/j.1460-2075.1988.tb03332.x

499 23. Newcomb LL, Diderich JA, Slattery MG, Heideman W. Glucose Regulation of *Saccharomyces*
500 *cerevisiae* Cell Cycle Genes. Eukaryot Cell. févr 2003;2(1):143-9. doi:10.1128/EC.2.1.143-
501 149.2003

502 24. Wu M, Newcomb L, Heideman W. Regulation of Gene Expression by Glucose inSaccharomyces
503 cerevisiae: a Role for ADA2and ADA3/NGG1. J Bacteriol. 15 août 1999;181(16):4755-60.
504 doi:10.1128/JB.181.16.4755-4760.1999

505 25. Fang O, Hu X, Wang L, Jiang N, Yang J, Li B, et al. Amn1 governs post-mitotic cell separation in
506 Saccharomyces cerevisiae. Barsh GS, éditeur. PLoS Genet. 1 oct 2018;14(10):e1007691.
507 doi:10.1371/journal.pgen.1007691

508 26. Laporte D, Jimenez L, Gouleme L, Sagot I. Yeast quiescence exit swiftness is influenced by cell
509 volume and chronological age. Microb Cell. 5 févr 2018;5(2):104-11.
510 doi:10.15698/mic2018.02.615

511 27. Courchesne WE, Kunisawa R, Thorner J. A putative protein kinase overcomes pheromone-
512 induced arrest of cell cycling in S. cerevisiae. Cell. 22 sept 1989;58(6):1107-19. doi:10.1016/0092-
513 8674(89)90509-6

28. Madhani HD, Styles CA, Fink GR. MAP Kinases with Distinct Inhibitory Functions Impart Signaling Specificity during Yeast Differentiation. Cell. nov 1997;91(5):673-84. doi:10.1016/S0092-8674(00)80454-7

29. Madhani HD, Galitski T, Lander ES, Fink GR. Effectors of a developmental mitogen-activated protein kinase cascade revealed by expression signatures of signaling mutants. Proc Natl Acad Sci USA. 26 oct 1999;96(22):12530-5. doi:10.1073/pnas.96.22.12530

30. Bozdag GO, Libby E, Pineau R, Reinhard CT, Ratcliff WC. Oxygen suppression of macroscopic multicellularity. Nat Commun. 14 mai 2021;12(1):2838. doi:10.1038/s41467-021-23104-0

31. Kapsetaki SE, West SA. The costs and benefits of multicellular group formation in algae*. Evolution. juin 2019;73(6):1296-308. doi:10.1111/evo.13712

32. Barrere J, Nanda P, Murray AW. Alternating selection for dispersal and multicellularity favors regulated life cycles. Current Biology. mai 2023;33(9):1809-1817.e3. doi:10.1016/j.cub.2023.03.031

33. Sherman F. [1] Getting started with yeast. In: Methods in Enzymology [Internet]. Elsevier; 1991 [cité 16 juin 2025]. p. 3-21. Disponible sur: https://linkinghub.elsevier.com/retrieve/pii/007668799194004V doi:10.1016/0076-6879(91)94004-V

34. Gietz D, Jean ASt, Woods RA, Schiestl RH. Improved method for high efficiency transformation of intact yeast cells. Nucl Acids Res. 1992;20(6):1425-1425. doi:10.1093/nar/20.6.1425

35. Gietz RD, Akio S. New yeast-Escherichia coli shuttle vectors constructed with in vitro mutagenized yeast genes lacking six-base pair restriction sites. Gene. déc 1988;74(2):527-34. doi:10.1016/0378-1119(88)90185-0

Figures

Figure 1

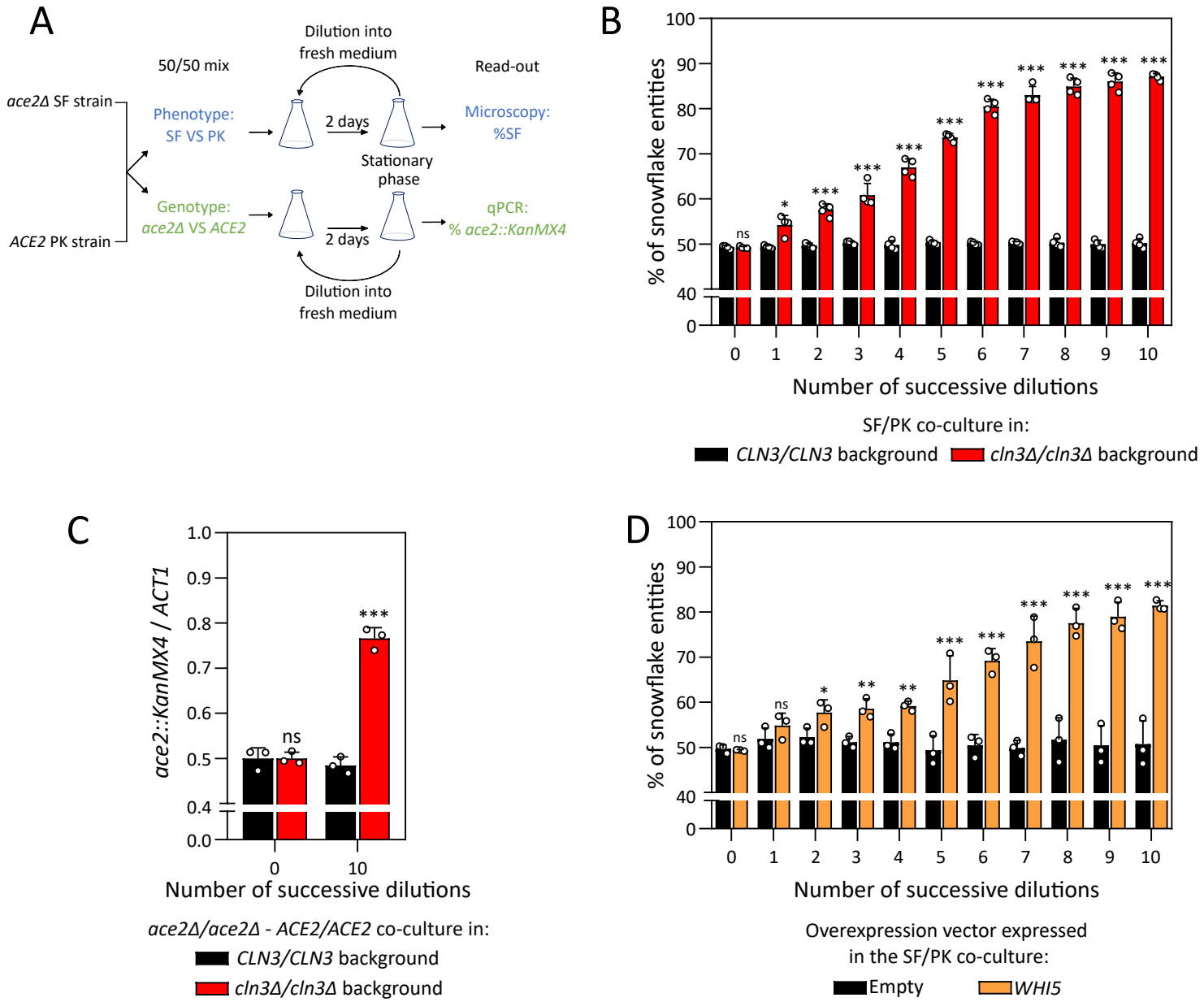
A
50/50 mix
Dilution into fresh medium
Read-out
ace2Δ SF strain
Phenotype: SF VS PK
2 days
Microscopy: %SF
Stationary phase
Genotype: ace2Δ VS ACE2
2 days
qPCR: % ace2::KanMX4
ACE2 PK strain
Dilution into fresh medium
B
% of snowflake entities
Number of successive dilutions
SF/PK co-culture in:
CLN3/CLN3 background
cln3Δ/cln3Δ background
C
ace2::KanMX4 / ACT1
Number of successive dilutions
ace2Δ/ace2Δ - ACE2/ACE2 co-culture in:
CLN3/CLN3 background
cln3Δ/cln3Δ background
D
% of snowflake entities
Number of successive dilutions
Overexpression vector expressed in the SF/PK co-culture:
Empty
WHI5

Figure 1 - figure supplement 1

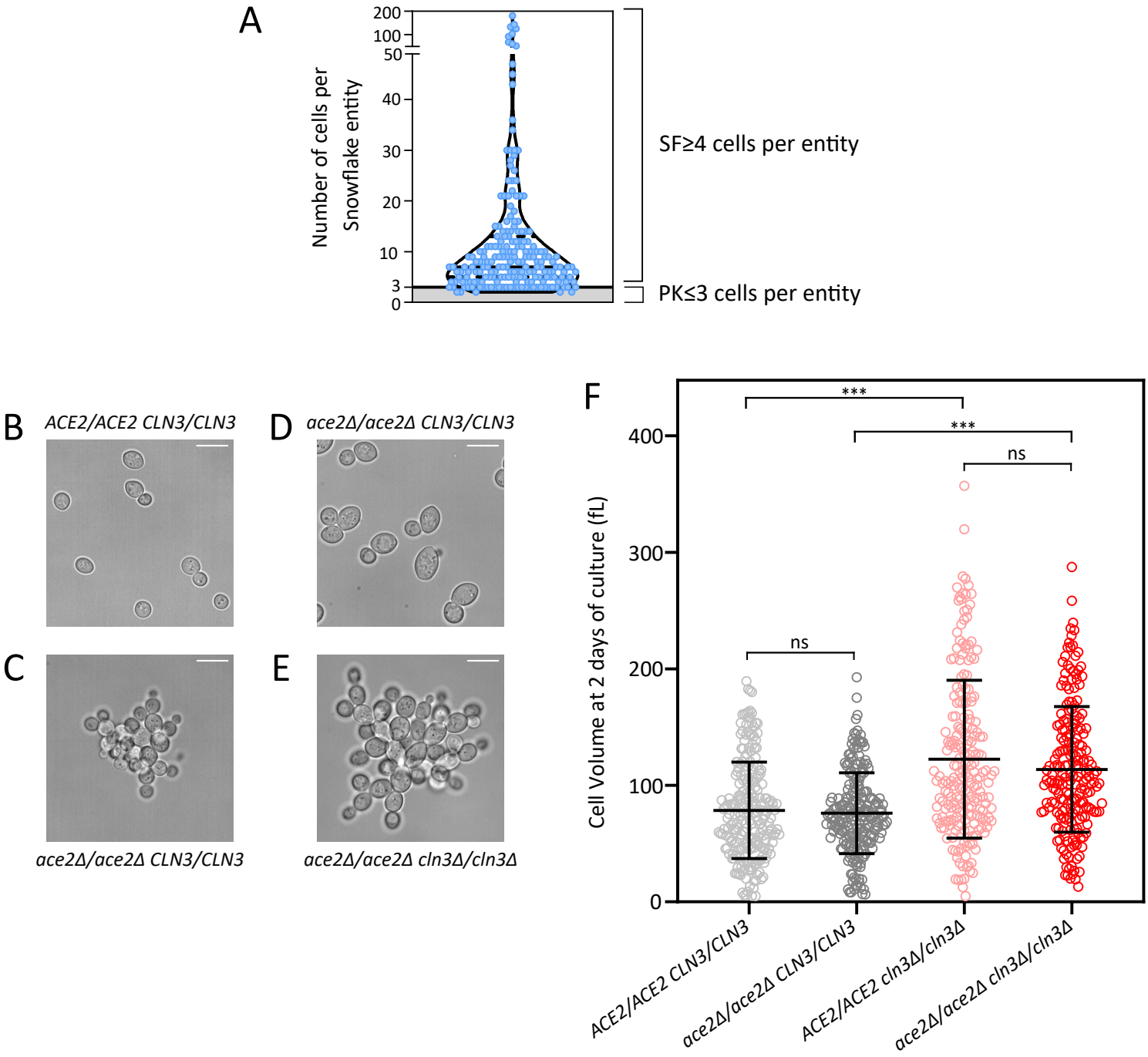

540 **Figure 1. Competition experiments. (A)** Experimental set-up of the co-culture competition
541 experiments between *ace2/ace2* and *ACE2/ACE2* strains. A 50/50 mix of the two strains based either
542 on phenotype (snowflake vs planktonic, microscopy) or on genotype (*ace2* vs *ACE2,* qPCR) was
543 inoculated in SDcasaWAU liquid medium. The resulting co-culture was grown for 2 days until stationary
544 phase was reached and then diluted in new SDcasaWAU medium. For each dilution step, the
545 proportion of the snowflake phenotype or *ace2* genotype was determined (by microscopy or qPCR
546 respectively). **(B)** Evolution of the percentage of snowflake entities during independent co-culture
547 competitions between *ace2/ace2* and *ACE2/ACE2* strains, either *cln3/cln3* (red bars) or *CLN3/CLN3*
548 (black bars) (N=4, n>250, mean ± SD, ns p>0.05, *p<0.05, ***p<0.001). The percentage of snowflakes
549 is statistically compared between *CLN3/CLN3* and *cln3/cln3* co-cultures at each dilution round, using a
550 Fisher's exact test. **(C)** The proportion of *ace2/ace2* genotype was monitored by qPCR in independent
551 competitions in *cln3/cln3* (red bars) and *CLN3/CLN3* (black bars) backgrounds. The *ACT1* locus,
552 amplified in all the cells of the population, was used to normalize the proportion of *ace2* cells in the
553 co-culture cell population (N=3, mean ± SD, unpaired t-test, Welch correction, ns p>0.05, ***p<0.001).
554 **(D)** Evolution of the percentage of snowflake entities during independent co-culture competitions
555 between *ace2/ace2* and *ACE2/ACE2* strains overexpressing *WHI5* (orange bars) or not (black bars)
556 (N=3, n>235, mean ± SD, Fisher's exact test, ns p>0.05, *p<0.05, **p<0.005, ***p<0.001).

557 **Figure supplement 1. (A)** Number of cells per Snowflake entity determined by counting the number
558 of *HTB1-CFP* positive nuclei per Snowflake entity. **(B-E)** Representative images of *CLN3/CLN3* strains,
559 either *ACE2/ACE2* **(B)** or *ace2/ace2* **(C)**, and cln3/cln3 strains, either *ACE2/ ACE2* **(D)** or *ace2/ace2* **(E)**.
560 Bars are 10 µm. **(F)** Cell volume measured at 2 days of culture (error bars ± SD, unpaired t-test, Welch
561 correction, ***p<0.001, ns p>0.05).

Figure 2

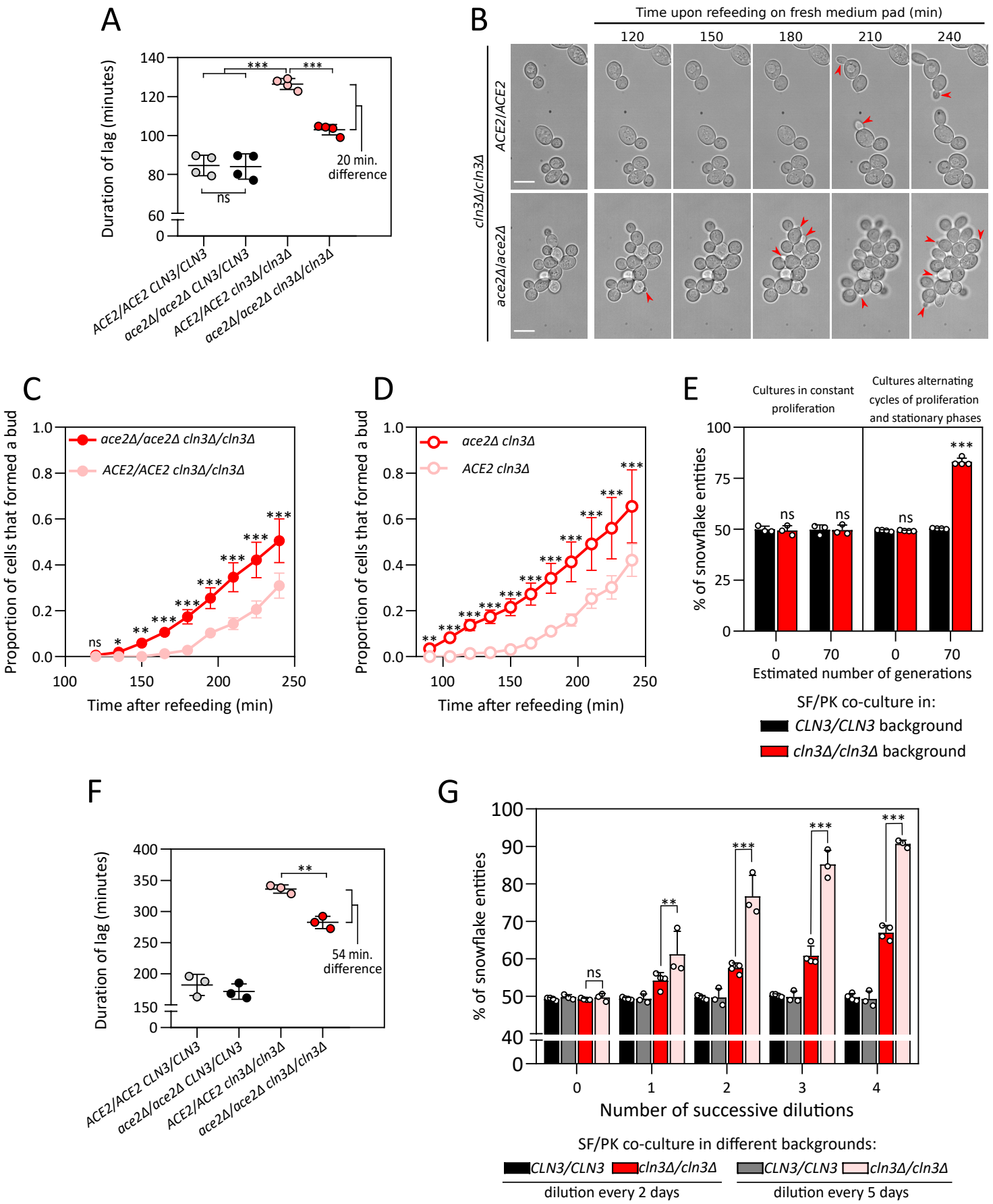
A
Duration of lag (minutes)
140
120
100
80
60
0
***
***
ns
20 min. difference
ACE2/ACE2 CLN3/CLN3
ace2Δ/ace2Δ CLN3/CLN3
ACE2/ACE2 cln3Δ/cln3Δ
ace2Δ/ace2Δ cln3Δ/cln3Δ
B
Time upon refeeding on fresh medium pad (min)
120
150
180
210
240
ACE2/ACE2
cln3Δ/cln3Δ
ace2Δ/ace2Δ
C
Proportion of cells that formed a bud
ace2Δ/ace2Δ cln3Δ/cln3Δ
ACE2/ACE2 cln3Δ/cln3Δ
Time after refeeding (min)
D
Proportion of cells that formed a bud
ace2Δ cln3Δ
ACE2 cln3Δ
Time after refeeding (min)
E
Cultures in constant proliferation
Cultures alternating cycles of proliferation and stationary phases
% of snowflake entities
Estimated number of generations
SF/PK co-culture in:
CLN3/CLN3 background
cln3Δ/cln3Δ background
F
Duration of lag (minutes)
54 min. difference
ACE2/ACE2 CLN3/CLN3
ace2Δ/ace2Δ CLN3/CLN3
ACE2/ACE2 cln3Δ/cln3Δ
ace2Δ/ace2Δ cln3Δ/cln3Δ
G
% of snowflake entities
Number of successive dilutions
SF/PK co-culture in different backgrounds:
CLN3/CLN3
cln3Δ/cln3Δ
CLN3/CLN3
cln3Δ/cln3Δ
dilution every 2 days
dilution every 5 days

Figure 2 - figure supplement 1

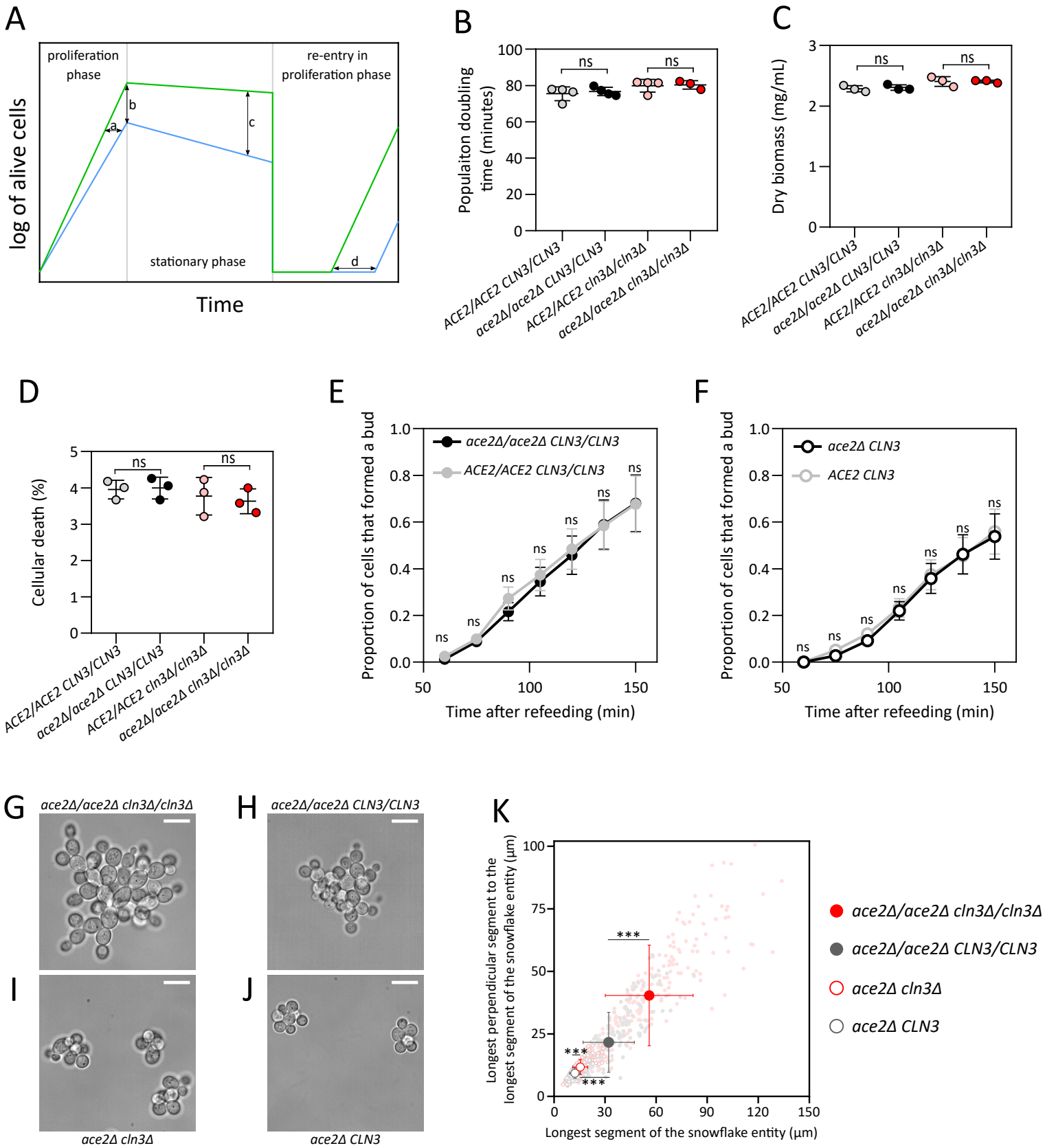

562 **Figure 2. Quiescence exit efficiency explains the results of competition experiments. (A)** Lag phase
563 duration after cell 2-day old population refeeding with SDCasaWAU medium. The optical density at
564 600nm was followed after population refeeding for 4 independent experiments. The mean and the SD
565 are indicated together with an unpaired t-test, Welch correction, ns p>0.05, ***p<0.001. **(B)**
566 Representative image series of *cln3/cln3* cells either *ace2/ace2* or *ACE2/ACE2* after refeeding of 2 days
567 cultures on a SDCasaWAU medium containing microscope pad. Arrows point to emerging buds. Bars
568 are 10µm. **(C)** Proportion of *cln3/cln3* cells that have formed a new bud after refeeding on a
569 SDCasaWAU medium containing microscope pad of either *ace2/ace2* or *ACE2/ACE2* 2 days cultures
570 (N=3, n>101, Fisher's exact test, mean ± SD, ns p>0.05, *p<0.05, **p<0.005, ***p<0.001). **(D)** Same as
571 C in a *cln3* haploid background (N=3, n>100, mean ± SD, Fisher's exact test, **p<0.005, ***p<0.001).
572 **(E)** Percentage of snowflake entities observed in independent co-cultures of *ace2/ace2* and *ACE2/ACE2*
573 strains. Cultures either went through cycles of proliferation and stationary phase as described in Fig1A
574 (right panel), or maintained in constant exponential phase (left panel) (N>3, n>208, mean ± SD, Fisher's
575 exact test, ns p>0.05). **(F)** Same as A except that the refeeding was done after a culture of 5 days (N=3,
576 mean ± SD, unpaired t-test, Welch correction, **p<0.005). **(G)** Percentage of snowflake entities
577 observed in independent co-cultures of *ace2/ace2* and *ACE2/ACE2* strains diluted every two days (red
578 and black bars) or every five days (grey and pink bars) (N≥3, n>700, mean ± SD, Fisher's exact test, ns
579 p>0.05, **p<0.005, ***p<0.001).

580 **Figure supplement 1**. **(A)** Theoretical diagram showing the various phenomena that can explain, either
581 alone or combined, how one subpopulation can outcompete another subpopulation in a co-culture.
582 One subpopulation may divide more rapidly in exponential phase (a), may have a higher yield (b), may
583 undergo less cell death during stationary phase (c) or may re-enter proliferation phase faster after
584 refeeding (d). **(B)** Doubling time of populations in proliferation phase. Independent cultures (N>3) were
585 maintained in constant proliferation phase for more than 24 hours, then the optical density at 600 nm
586 was measured every 15 minutes for 8 hours (mean ± SD, unpaired t-test, Welch correction, ns p>0.05).
587 **(C-D)** The dry biomass determined by filtration (**C**, N=3, mean ± SD, unpaired t-test, Welch correction,

588 ns p>0.05) and the percentage of dead cells stained with ethylene blue (**D**, N=3, n>280, mean ± SD,
589 Fisher's exact test, ns p>0.05,) were also measured for 2 days stationary phase cultures. **(E)** Proportion
590 of *CLN3/CLN3* cells that have formed a new bud after refeeding on a SDCasaWAU medium containing
591 microscope pad of either *ace2/ace2* or *ACE2/ACE2* 2 days cultures (N=3, n>101, Fisher's exact test,
592 mean ± SD, ns p>0.05). **(F)** Proportion of *CLN3* cells that have formed a new bud after refeeding on a
593 SDCasaWAU medium containing microscope pad of either *ace2* or *ACE2* 2 days cultures (N=3, n>91,
594 Fisher's exact test, mean ± SD, ns p>0.05). **(G-J)** Representative images of diploid *ace2/ace2* snowflakes
595 either *cln3/cln3* (**G**) or *CLN3/CLN3* (**H**), and haploid *ace2* snowflakes either *cln3* (**I**) or *CLN3* (**J**). Bars are
596 10 µm. **(K).** Size distribution of snowflakes in haploid (empty circles) or diploids (plain circles)
597 backgrounds, either *CLN3* (black) or *cln3* (red). Size is estimated by measuring both the longest
598 segment of the snowflake entity and the longest segment perpendicular to the first one (N=3, n>72).
599 We compared the length of each segment independently with an unpaired t-test with a Welch
600 correction (error bars ± SD, unpaired t-test, Welch correction, ***p<0.001, account for both segment).

Figure 3

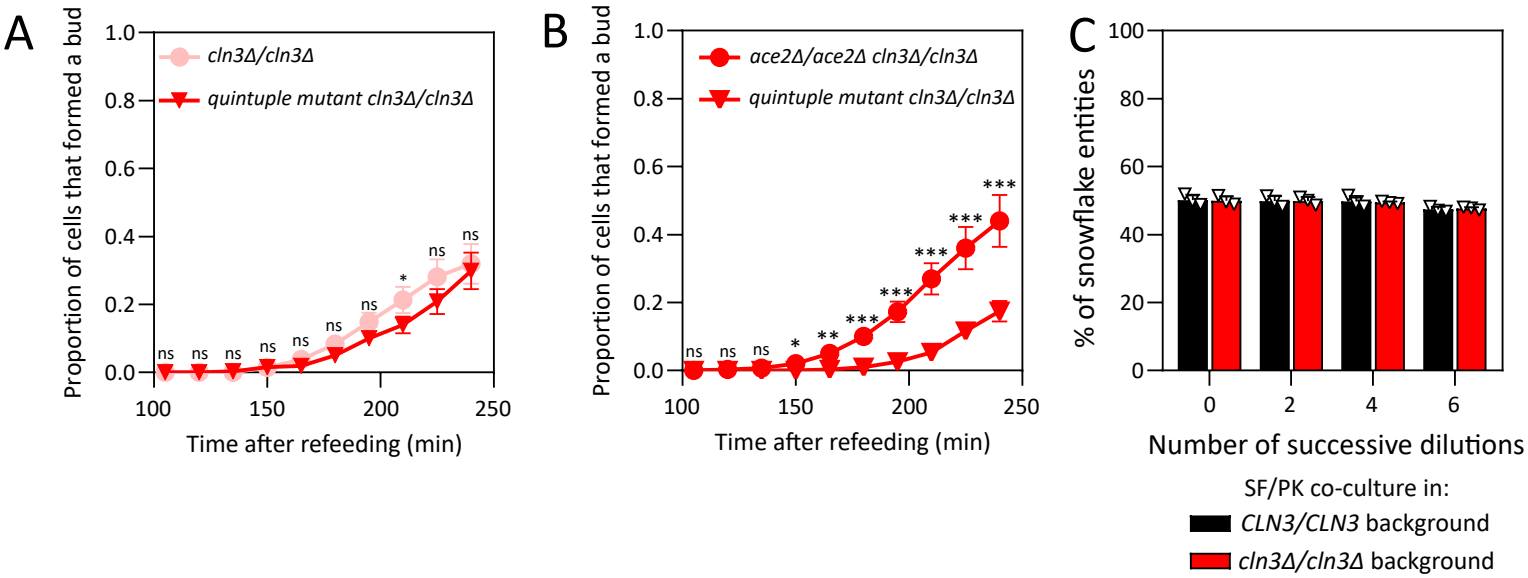
A
Proportion of cells that formed a bud
1.0
0.8
0.6
0.4
0.2
0.0
cln3Δ/cln3Δ
quintuple mutant cln3Δ/cln3Δ
ns
*
100
150
200
250
Time after refeeding (min)
B
Proportion of cells that formed a bud
ace2Δ/ace2Δ cln3Δ/cln3Δ
quintuple mutant cln3Δ/cln3Δ
ns
*
**
***
Time after refeeding (min)
C
% of snowflake entities
100
80
60
40
20
0
0
2
4
6
Number of successive dilutions
SF/PK co-culture in:
CLN3/CLN3 background
cln3Δ/cln3Δ background

Figure 3 - figure supplement 1

A

Quintuple mutant strain

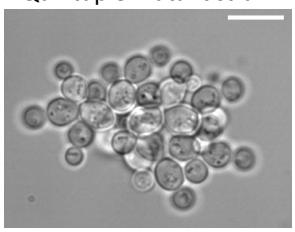

B

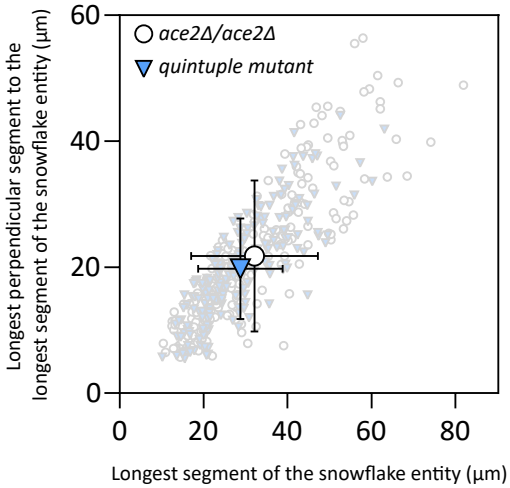

C

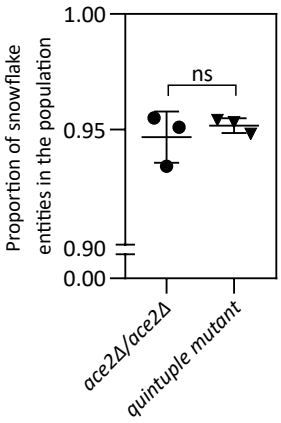

601 **Figure 3. Quintuple *cts1, dse2, dse4, egt2, scw11* mutant strains do not rescue the quiescence-exit**
602 **default associated with *cln3* and are not selected in competition experiments. (A)** Proportion of
603 *cln3/cln3* cells, either quintuple mutant or WT, that formed a new bud after refeeding of 2 days
604 cultures on a SDCasaWAU medium containing microscope pad (N=3, n>102, mean ± SD, Fisher's exact
605 test, ns p>0.05, *p<0.05). **(B)** Proportion of *cln3/cln3* cells, either quintuple mutant or *ace2/ace2*, that
606 formed a new bud after refeeding of 2 days cultures on a SDCasaWAU medium containing microscope
607 pad (N=3, n>75, mean ± SD, Fisher's exact test, ns p>0.05, *p<0.05, **p<0.005, ***p<0.001). **(C)**
608 Evolution of the percentage of snowflake entities during independent co-culture competitions
609 between quintuple mutant and WT strains either *cln3/cln3* (red bars) or *CLN3/CLN3* (black bars) (N=3,
610 n>250, mean ± SD, Fisher's exact test).

611 **Figure supplement 1. Snowflake characterization of quintuple mutant strains. (A)** Representative
612 image of the quintuple mutant strain. Bar is 10µm. **(B)** Size distribution of quintuple mutant (triangles)
613 or *ace2/ace2* (circles) snowflakes. Size is estimated by measuring both the longest segment of the
614 snowflake entity and the longest segment perpendicular to the first one. We compared the length of
615 each segment independently with an unpaired t-test with a Welch correction (N=3, n>60, mean ± SD).
616 **(C)** Proportion of snowflake entities in a population of quintuple mutant or *ace2/ace2* strains (N=3,
617 n>201, mean ± SD, Fisher's exact test, ns p>0.05).

Figure 4

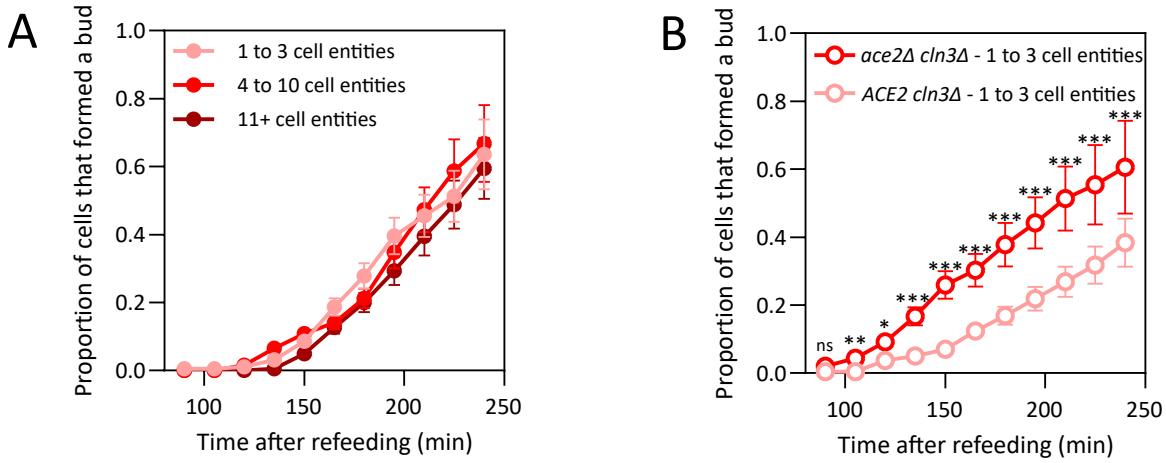
A
Proportion of cells that formed a bud
1.0
0.8
0.6
0.4
0.2
0.0
1 to 3 cell entities
4 to 10 cell entities
11+ cell entities
100
150
200
250
Time after refeeding (min)
B
Proportion of cells that formed a bud
1.0
0.8
0.6
0.4
0.2
0.0
ace2Δ cln3Δ - 1 to 3 cell entities
ACE2 cln3Δ - 1 to 3 cell entities
ns
**
*
***
***
***
***
***
***
100
150
200
250
Time after refeeding (min)

Figure 4 - figure supplement 1

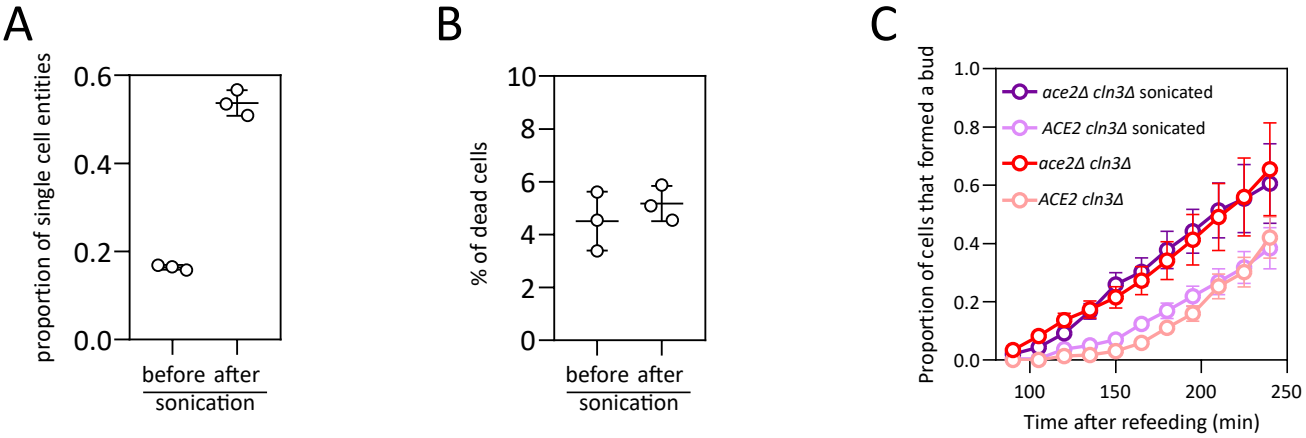

618 **Figure 4. Rescue of the quiescence-exit default associated with *cln3* depends on the *ace2* mutation**
619 **and not on the Snowflake phenotype. (A)** A 2-day *ace2/ace2 cln3/cln3* culture was sonicated and refed
620 onto a fresh SDCasaWAU microscope pad. The proportion of cells that formed a new bud after
621 refeeding on a SDCasaWAU medium containing microscope pad was assessed within different
622 multicellular size ranges (N=3, n>184, mean ± SD, Fisher's exact test). **(B)** 2-day *cln3* cultures, either
623 *ace2* or *ACE2*, were sonicated and refed onto a fresh SDCasaWAU microscope pad. Within entities
624 formed of 1 to 3 cells, the proportion of cells that formed a new bud after refeeding on a SDCasaWAU
625 medium containing microscope pad was assessed (N=3, n>63, mean ± SD, Fisher's exact test, ns p>0.05,
626 *p<0.05, **p<0.005, ***p<0.001).

627 **Figure supplement 1**. **Effect of sonication on SF phenotype, cell death and quiescence exit**. **(A-B)** The
628 effect of sonication bath on an *ace2* culture was assessed by measuring the proportion of single cell
629 entities (**A**, N=3, n>212) and the percentage of dead cells (**B**, N=3, n>207) in the population before and
630 after the culture was sonicated. **(C)** Proportion of *cln3* cells, either *ace2* or *ACE2*, and either sonicated
631 or not, that formed a new bud after refeeding of 2 days cultures on a SDCasaWAU medium containing
632 microscope pad (N=3, n>63, Fisher's exact test, mean ± SD).

Figure 5

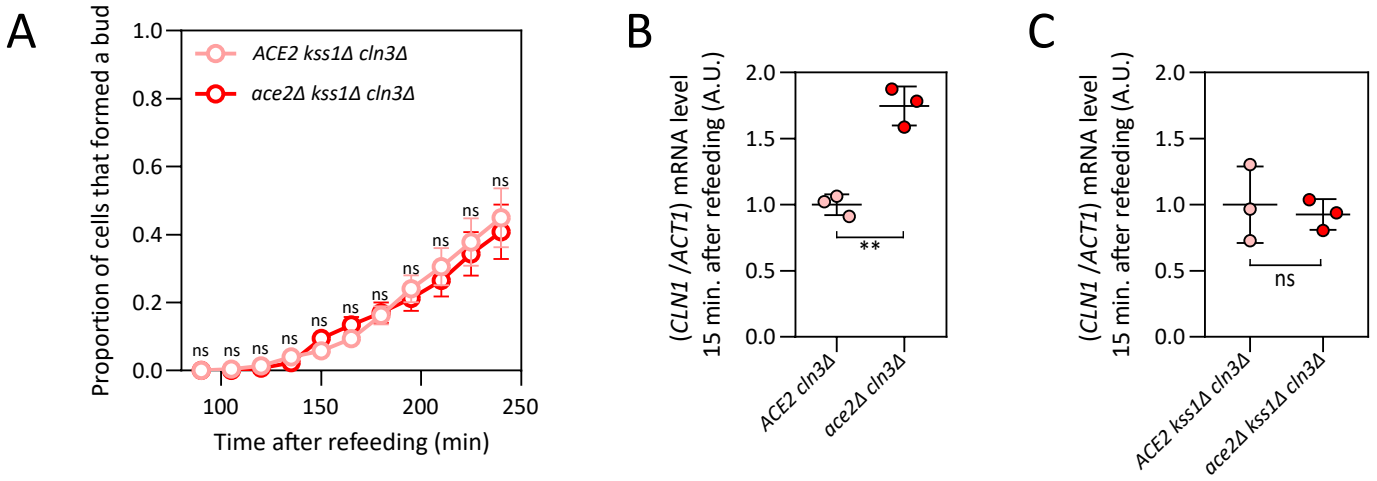
A
Proportion of cells that formed a bud
1.0
0.8
0.6
0.4
0.2
0.0
ACE2 kss1Δ cln3Δ
ace2Δ kss1Δ cln3Δ
ns
100
150
200
250
Time after refeeding (min)
B
(CLN1 /ACT1) mRNA level
15 min. after refeeding (A.U.)
2.0
1.5
1.0
0.5
0.0
**
ACE2 cln3Δ
ace2Δ cln3Δ
C
(CLN1 /ACT1) mRNA level
15 min. after refeeding (A.U.)
ns
ACE2 kss1Δ cln3Δ
ace2Δ kss1Δ cln3Δ

633 **Figure 5. Rescue of the quiescence-exit default associated with *cln3* is dependent on the Kss1 MAP**
634 **kinase, which favors transcription of the *CLN1* cyclin gene. (A)** Proportion of *cln3 kss1* cells, either
635 *ace2* or *ACE2*, that formed a new bud after refeeding of 2-day cultures on a fresh SDCasaWAU medium
636 containing microscope pad (N=3, n>86, mean ± SD, Fisher's exact test, ns p>0.05). **(B)** Ratio of *CLN1*
637 mRNA level and *ACT1* mRNA level, determined by RT-qPCR, 15 minutes after refeeding of 2 days *cln3*
638 cultures, either *ace2* or *ACE2* (N=3, mean ± SD, unpaired t-test, Welch correction, **p<0.005). **(C)** Ratio
639 of *CLN1* mRNA level and *ACT1* mRNA level, determined by RT-qPCR, 15 minutes after refeeding of 2-
640 day *kss1 cln3* cultures, either *ace2* or *ACE2* (N=3, mean ± SD, unpaired t-test, Welch correction, ns
641 p>0.05).

Figure 6

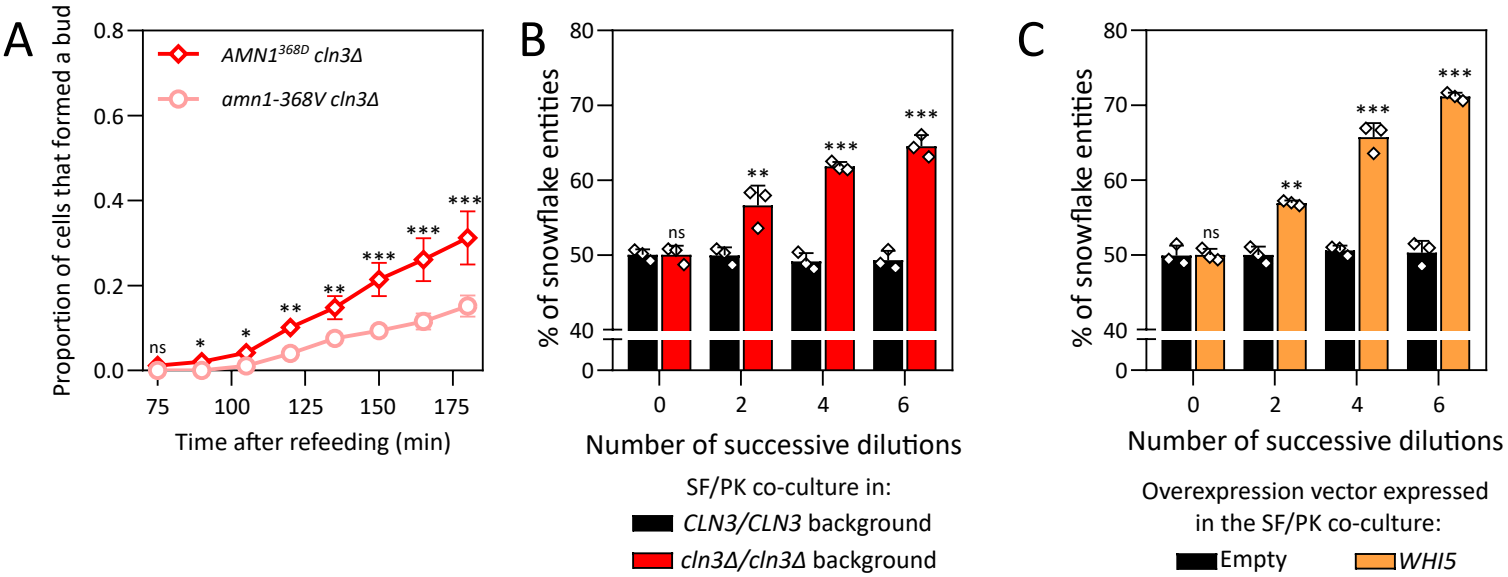
A
Proportion of cells that formed a bud
0.8
0.6
0.4
0.2
0.0
AMN1368D cln3Δ
amn1-368V cln3Δ
ns
*
*
**
**
***
***
***
75
100
125
150
175
Time after refeeding (min)
B
% of snowflake entities
80
70
60
50
40
0
ns
**
***
***
0
2
4
6
Number of successive dilutions
SF/PK co-culture in:
CLN3/CLN3 background
cln3Δ/cln3Δ background
C
% of snowflake entities
80
70
60
50
40
0
ns
**
***
***
0
2
4
6
Number of successive dilutions
Overexpression vector expressed
in the SF/PK co-culture:
Empty
WHI5

Figure 6 - figure supplement 1

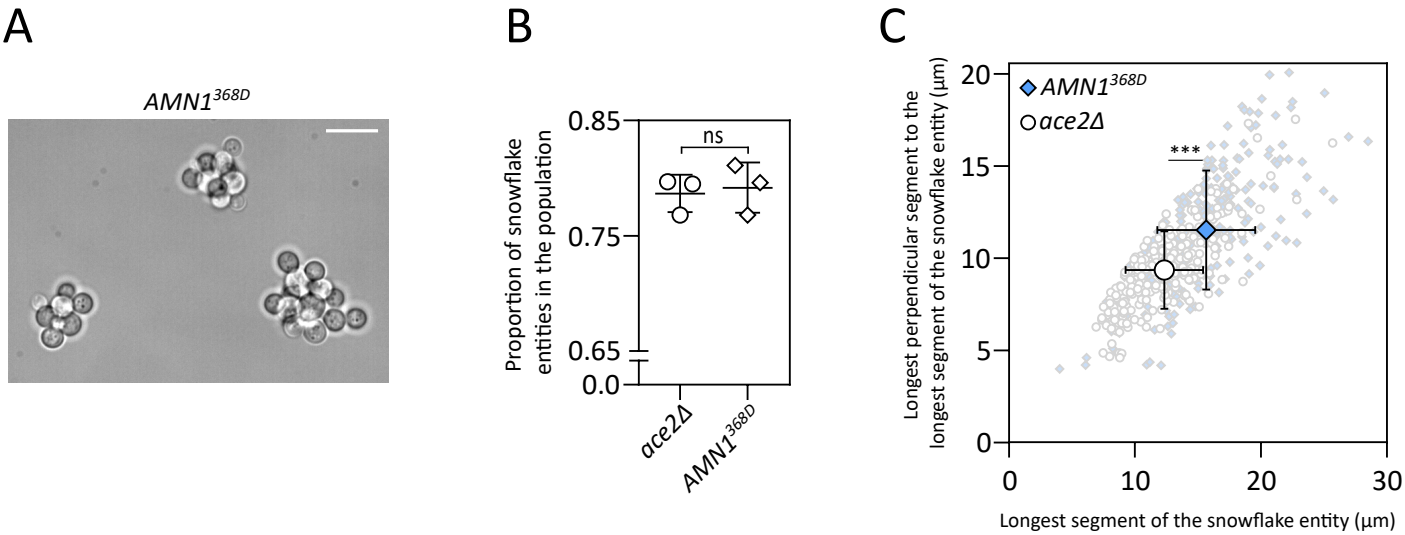

642 **Fig 6. Quiescence exit efficiency and selection in competition experiments of Snowflake *AMN1^{368D}***
643 **strains. (A)** Proportion of *cln3* cells, either *AMN1^{368D}* or *amn1-368V*, that formed a new bud after
644 refeeding of 2 days cultures on a fresh SDCasaWAU medium containing microscope pad (N=3, n>77,
645 mean ± SD, Fisher's exact test, ns p>0.05, *p<0.05, **p<0.005, ***p<0.001). **(B)** Evolution of the
646 percentage of snowflake entities during independent co-culture competitions between *AMN1^{368D}* and
647 *amn1-368V* strains, either *cln3/cln3* (red bars) or *CLN3/CLN3* (black bars) (N=3, n>252, mean ± SD,
648 Fisher's exact test, ns p>0.05, **p<0.005, ***p<0.001). **(C)** Evolution of the percentage of snowflake
649 entities during independent co-culture competitions between *AMN1^{368D}* and *amn1-368V* strains
650 overexpressing *WHI5* (orange bars) or not (black bars) (N=3, n>302, Fisher's exact test, ns p>0.05,
651 **p<0.005, ***p<0.001).

652 **Figure supplement 1. Snowflake characterization of *AMN1^{368D}* strains. (A)** Representative image of
653 the *AMN1^{368D}* strain. Bar is 10µm. **(B)** Proportion of snowflake entities in populations of *AMN1^{368D}* or
654 *ace2* haploid strains (N=3, n>219, mean ± SD, Fisher's exact test, ns p>0.05). **(C)** Size distribution of
655 *AMN1^{368D}* (diamond) or *ace2* (circle) snowflakes. Size is estimated by measuring both the longest
656 segment of the snowflake entity and the longest segment perpendicular to the first one (N=3, n>74,
657 mean ± SD, unpaired t-test, Welch correction, ***p<0.001, account for both segment).

Figure 7

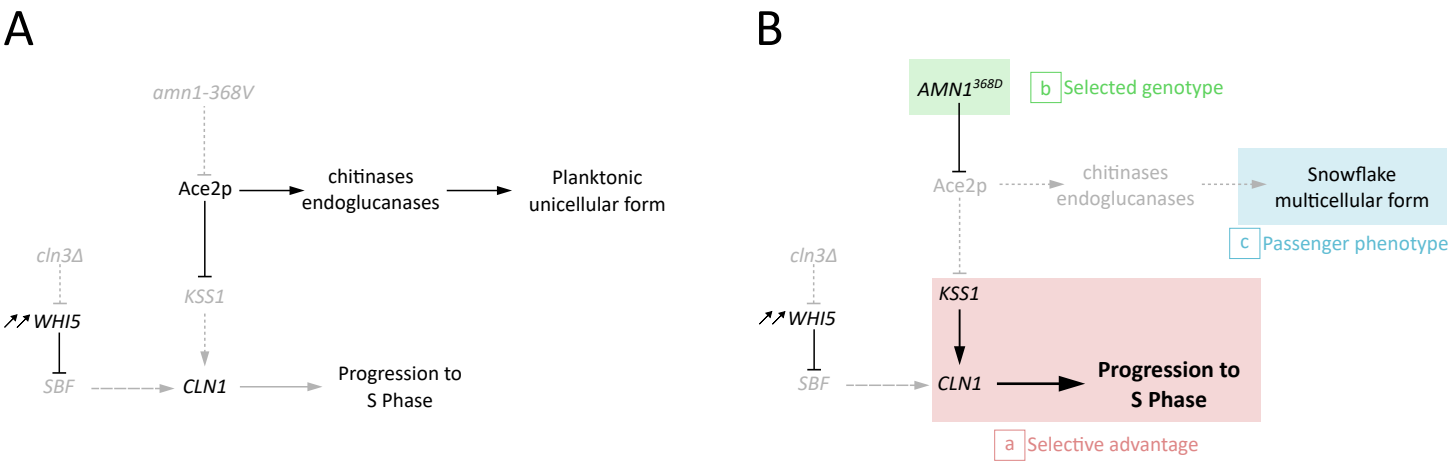
A
amn1-368V
Ace2p
chitinases
endoglucanases
Planktonic
unicellular form
cln3Δ
KSS1
↗↗WHI5
SBF
CLN1
Progression to
S Phase
B
AMN1368D
b Selected genotype
Ace2p
chitinases
endoglucanases
Snowflake
multicellular form
c Passenger phenotype
cln3Δ
KSS1
↗↗WHI5
SBF
CLN1
Progression to
S Phase
a Selective advantage

658 **Fig 7. Model explaining the selection of the Snowflake phenotype as a passenger phenotype.** In
659 strains expressing the non- functional *amn1-368V* allele **(A)**, a default in quiescence exit after refeeding
660 was observed in a *cln3* mutant. In non-laboratory strains **(B)**, the functional *AMN1*^{368D} allele leads to
661 degradation of Ace2p, which can no longer repress the expression of the Kss1 Map kinase. Kss1p favors
662 the transcription of *CLN1*, which would favor progression to S phase and partially suppress the default
663 in quiescence exit associated with the *cln3* mutation. This observed selective advantage (a) leads to
664 the selection of *AMN1*^{368D} genotype (b), and because of the pleiotropy of Ace2p transcription factor,
665 to the selection of the Snowflake multicellular phenotype as a passenger phenotype (c).